Title
SURFACE ASPECTS OF HYDROGEN PHOTOGENERATION OF TITANIUM OXIDES

Authors
Wagner, F.T.
Ferrer, S.
Somorjai, G.A.

Publication Date
1980-07-01

LBL-11456 c.2

Lawrence Berkeley Laboratory
UNIVERSITY OF CALIFORNIA

Materials & Molecular Research Division

To be presented at the American Chemical Society Symposium on "Photoeffects at Semiconductor-Electrolyte Interfaces, Golden, CO, October 15, 1980

SURFACE ASPECTS OF HYDROGEN PHOTOGENERATION ON TITANIUM OXIDES

F.T. Wagner, S. Ferrer, and G.A. Somorjai

July 1980

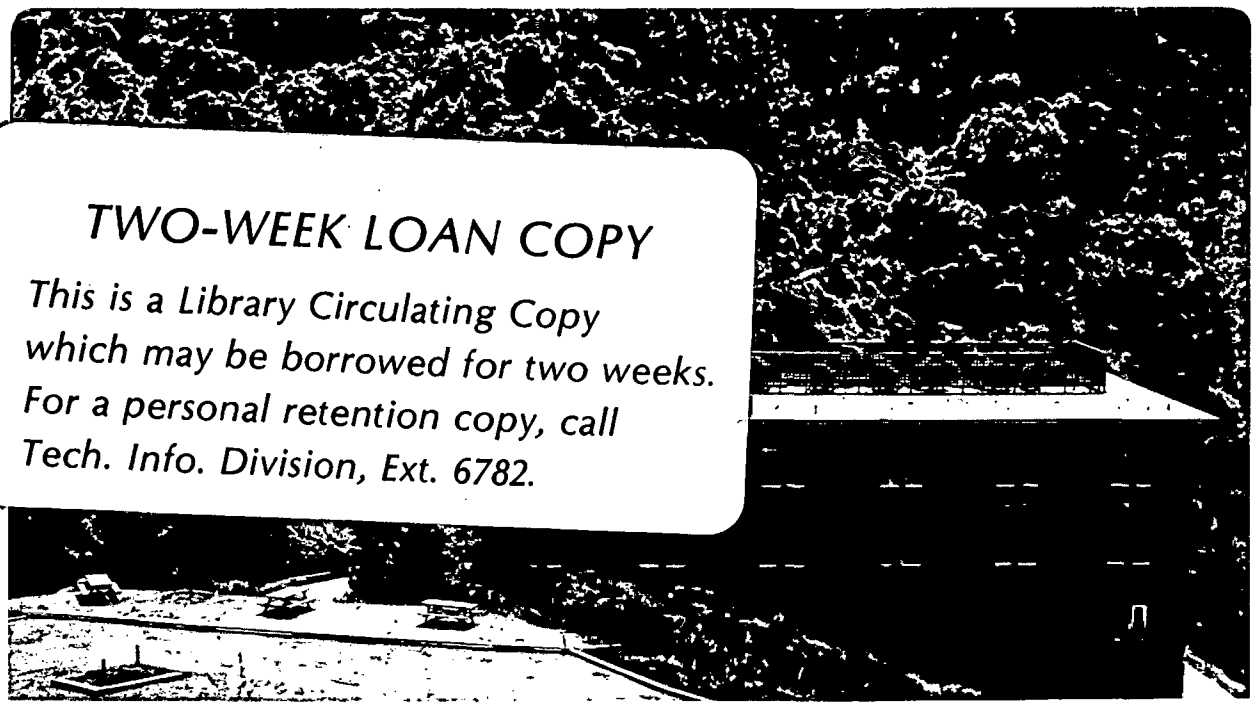

Prepared for the U.S. Department of Energy under Contract W-7405-ENG-48

DISCLAIMER

SURFACE ASPECTS OF HYDROGEN PHOTOGENERATION ON TITANIUM OXIDES

F.T. Wagner, S. Ferrer, and G.A. Somorjai

Materials and Molecular Research Division, Lawrence Berkeley Laboratory, and Department of Chemistry, University of California, Berkeley, CA 94720, USA

Strontium titanate and titanium dioxide have received considerable attention as materials for photoanodes and photocatalysts in the dissociation of water (1,2,3), and in other photoassisted reactions. Knowledge of how the surface composition and electronic structure of these materials change under illumination when in contact with gases or liquid electrolytes is essential if detailed understanding of the mechanisms of semiconductor photochemistry is to be achieved. Although these wide bandgap oxides do not exhibit gross photocorrosion under most reaction conditions (2) and would appear less susceptable to possible Fermi-level pinning than many semiconductors with smaller bandgaps (4), more subtle surface chemical effects have been documented. Evidence for photocorrosion (5,6,7), surface-state mediation of electron and hole transfer to electrolyte species (8,9), and the dependence of quantum efficiencies on surface preparation techniques (10), indicate important roles for surface species on wide bandgap materials.

Most detailed studies of water photodissociation on $SrTiO_3$ and TiO_2 have concentrated on photoelectrochemical cells (PEC cells) operating under conditions of optimum efficiency, that is with an external potential applied between the photoanode and counterelectrode. We have become interested in understanding and improving reaction kinetics under conditions of zero applied potential. Operation at zero applied potential permits simpler electrode configurations (11) and is essential to the development of photochemistry at the gas-semiconductor interface. Reactions at the gas-sold, rather than liquid-solid, interface might permit the use of materials which photocorrode in aqueous electrolyte. The gas-solid interface is also more amenable to the application of ultrahigh vacuum surface analytical techniques.

In this paper the hydroxide concentration dependence of the rate of hydrogen production in $SrTiO_3$ systems (12) is discussed in light of surface analytical results. The surface elemental composition before and after illumination in various aqueous electrolytes has been monitored with Auger electron spectroscopy

and is compared with the composition obtained by ultrahigh vacuum surface preparation techniques. Auger spectroscopy, while less sensitive than photoelectron spectroscopies to subtle changes in the oxidation states of surface species, is more easily applied to the imperfectly clean surfaces obtained in basic aqueous electrolytes using present technology. Carbon and silicon impurities are found on surfaces exposed to electrolytes; the carbonaceous species have some filled states which may make them effective for the mediation of charge transfer across the interface. The effects of surface platinization on photoactivity are discussed and evidence for a thermal reaction between Pd and TiO_2 surfaces is given. (13)

A hydrogen-producing stoichiometric photoreaction occurs between pre-reduced $SrTiO_3$ and $\frac{1}{10}^{-7}$ Torr water vapor.(14) At these low pressures surface Ti^{3+} and hydroxyl species can be observed by photoelectron spectroscopies. Comparison of the reaction conditions required for hydrogen photogeneration from low pressure water vapor and from aqueous electrolyte allows some speculation as to the roles of hydroxyl species.

II. Experimental

II.1. Liquid-solid Interface Experiments. Single crystal wafers for experiments in liquid electrolyte were cut to within 2% of the (111) face and etched 3-5 minutes in molten NaOH held in a gold lined crucible. Wafers were then rinsed in water, soaked 5 minutes in aqua regia, rinsed, soaked 5 minutes in high purity 35% aqueous NaOH (Apache SP 7329), rinsed in 7M-Ω triply distilled water, and air dried.

Liquid phase hydrogen photogeneration experiments were carried out with a gas chromatographic detection system described in more detail elsewhere.(12) Crystals rested in a 2-10 ml pool of electrolyte within a borosilicate glass vacuum flask. The detection system was sensitive to rates of at least $5x10^{15}$ molecules H_2/hr-cm^2 $SrTiO_3$ (≡5 monolayers/hr), but slow rates of oxygen production could not be followed. A 500W high pressure mercury lamp provided a flux of bandgap photons of $10^{16}cm^{-2}s^{-1}$.

The electrolyte for most experiments was compounded from reagent-grade materials and low conductivity water. However, in some experiments high purity (Apache SP7329 35% NaOH) or ultrapurity (Alfa 87864 30% NaOH) solutions were employed. Glassware for these experiments was prepared by soaking in 1:1 H_2SO_4:HNO_3, thoroughly rinsing in 7M-Ω water, and rinsing in the electrolyte to be used.

After being illuminated, the crystals were rinsed in low conductivity water, allowed to dry in air, and transferred into either a Physical Electronics 590 scanning Auger microprobe or into a UHV chamber equipped with a sample enetry lock, a Varian cylindrical mirror Auger analyzer, and a glancing incidence electron gun. Unless otherwise noted, crystals received no argon

and is compared with the composition obtained by ultrahigh vacuum surface preparation techniques. Auger spectroscopy, while less sensitive than photoelectron spectroscopies to subtle changes in the oxidation states of surface species, is more easily applied to the imperfectly clean surfaces obtained in basic aqueous electrolytes using present technology. Carbon and silicon impurities are found on surfaces exposed to electrolytes; the carbonaceous species have some filled states which may make them effective for the mediation of charge transfer across the interface. The effects of surface platinization on photoactivity are discussed and evidence for a thermal reaction between Pd and TiO_2 surfaces is given. (13)

A hydrogen-producing stoichiometric photoreaction occurs between pre-reduced $SrTiO_3$ and $\leq 10^{-7}$ Torr water vapor.(14) At these low pressures surface Ti^{3+} and hydroxyl species can be observed by photoelectron spectroscopies. Comparison of the reaction conditions required for hydrogen photogeneration from low pressure water vapor and from aqueous electrolyte allows some speculation as to the roles of hydroxyl species.

II. Experimental

II.1. Liquid-solid Interface Experiments. Single crystal wafers for experiments in liquid electrolyte were cut to within 2% of the (111) face and etched 3-5 minutes in molten NaOH held in a gold lined crucible. Wafers were then rinsed in water, soaked 5 minutes in aqua regia, rinsed, soaked 5 minutes in high purity 35% aqueous NaOH (Apache SP 7329), rinsed in 7M-Ω triply distilled water, and air dried.

Liquid phase hydrogen photogeneration experiments were carried out with a gas chromatographic detection system described in more detail elsewhere.(12) Crystals rested in a 2-10 ml pool of electrolyte within a borosilicate glass vacuum flask. The detection system was sensitive to rates of at least 5×10^{15} molecules H_2/hr-cm^2 $SrTiO_3$ ($\equiv$5 monolayers/hr), but slow rates of oxygen production could not be followed. A 500W high pressure mercury lamp provided a flux of bandgap photons of 10^{16}cm^{-2}s^{-1}.

The electrolyte for most experiments was compounded from reagent-grade materials and low conductivity water. However, in some experiments high purity (Apache SP7329 35% NaOH) or ultrapurity (Alfa 87864 30% NaOH) solutions were employed. Glassware for these experiments was prepared by soaking in 1:1 H_2SO_4:HNO_3, thoroughly rinsing in 7M-Ω water, and rinsing in the electrolyte to be used.

After being illuminated, the crystals were rinsed in low conductivity water, allowed to dry in air, and transferred into either a Physical Electronics 590 scanning Auger microprobe or into a UHV chamber equipped with a sample enetry lock, a Varian cylindrical mirror Auger analyzer, and a glancing incidence electron gun. Unless otherwise noted, crystals received no argon

sputtering, heating, or other cleaning treatments *in vacuo*.

II-2 Gas-solid Interface Experiments. Low pressure photoreactivity experiments were carried out in a UHV chamber previously described (15) equipped with an electron analyzer for Auger, photoelectron, and low resolution energy loss spectroscopies. D_2O vapor was admitted into the chamber through a variable leak valve. Photogenerated projects were detected with a UTI quadrupole mass spectrometer. The system was sensitive to H_2 generation rates as low a 0.3 monolayers/hour and had still higher sensitivity to oxygen.

A Physical Electronics single-pass CMA and a Phi 4-grid LEED Optics unit were used in the studies of metal films on TiO_2. Pd and Au films were evaporated from high-density alumina effusion sources.

$SrTiO_3$ and TiO_2 crystals for gas-phase studies were polished with 1μ diamond paste. "Pre-reduced" $SrTiO_3$ crystals were baked four hours in flowing hydrogen at 1270 K. TiO_2 crystals were reduced *in vacuo*. Clean surfaces were produced by Ar^+ bombardment and thermal annealing.

III. Results

III-1. Hydrogen production and surface stoichiometry. Hydrogen production was observed upon illumination of both stoichiometric and pre-reduced $SrTiO_3$ crystals in concentrated NaOH solutions. On metal-free crystals, rates of hydrogen production of 20 and up to 100 monolayers per hour (1 monolayer $\equiv 10^{15}$ molecules/cm^2 $SrTiO_3$) were commonly observed, corresponding to a quantum efficiency for photons with $h\nu > 3.2$ eV of 0.03-0.15%. Hydrogen production required bandgap radiation and could be maintained for hours (Figure 1). Rates of hydrogen evolution from platinum-free crystals in various electrolytes are listed in Table I. The rate of hydrogen production increases at high OH^- concentrations. (12) Similar rates were observed in 10M NaOH prepared from reagent-grade NaOH (heavy metal impurities 1 ppm sensitivity, Pt not reported). No hydrogen production was observed in 10M $NaClO_4$ compounded from a reagent containing 5 ppm heavy metal impurities.

Figure 2 shows Auger spectra of water-rinsed $SrTiO_3$ crystals (A) before illumination, (B) after illumination in 30% NaOH, and (C) after illumination in $NaClO_4$. (Spectrum D will be discussed later.) These spectra were taken with high beam current densities to allow more ready detection of impurities. Figure 3 shows Ti-O Auger spectra previously taken at low beam currents (<0.1μA) to minimize beam damage to the surface. The O(507 eV/Ti(380 eV) peak ratio of 2.6 is the same before and after hydrogen-producing illumination in 30% NaOH, but is higher (3.8) after illumination in 10M $NaClO_4$. Crystals illuminated in other electrolytes (pure water, 1 M H_2SO_4) gave spectra similar to those for illumination

in NaOH, although no hydrogen was produced. The Sr (66 eV)/Ti (380 eV) peak ratios before and after illumination in NaOH were also identical at 0.11. Oxygen mapping with the scanning Auger microprobe showed no regions of crystal illuminated in NaOH to be significantly depleted in oxygen, with a spatial resolution of $\sim 3\mu$. Thus no obvious development of macroscopic anodic and cathodic regions of the crystal occurs.

After crystal illumination, spectrophotometric examination of the electrolyte by the pertitanate method (16) showed no dissolved titanium with a sensitivity on the order of 10 monolayers. It appears that no irreversible change in the surface stoichiometry of constituent elements accompanies the slow photogeneration of hydrogen on metal-free crystals in aqueous NaOH. Although a change in stoichiometry occurred in $NaClO_4$, no such change occurs in other electrolytes which are also ineffective for hydrogen production.

III-2. Surface Contaminants. Most discussions of the role of surface states in the photochemistry of metal oxides have considered primarily states in the metal-oxygen system (8), induced by adsorption of major species from the electrolyte (17), or generated by intentional derivitization of the surface.(18) Surface impurities may also play a role in mediating charge transfer across the interface. A major carbon impurity (272 eV) was observed on all crystals contacted with liquid water. Typical carbon coverage was on the order of one monolayer, as estimated from Auger sensitivity factors based on TiO_2 and graphite. The carbon peak shape was more characteristic of graphite or a partially hydrogenated carbon layer than of a carbide (19) and the signal was too intense to be due to a carbonate.(20,21) Figure 9 shows Auger spectra of $SrTiO_3$ after Ar^+ sputtering (A), exposure to room air (B), and exposure to triply distilled water. Even on this highly reactive (22) sputtered surface the majority of carbon contamination arises from exposure to liquid water rather than to air.

UPS spectra of clean Ar^+ sputtered and *in vacuo* carbon-contaminated surfaces are shown in Figure 4. On the clean, sputtered surface a filled state due to Ti^{3+} lies 0.6 eV below the conduction band.(22) Carbon-induced filled states lie in a broad peak with considerable intensity between the valence band edge and the Ti^{3+} peak. Frank *et al.*(8) reported evidence that a state lying about 1.2 eV above the valence band mediates electron transfer from TiO_2 electrodes. Although these carbon states are as of now poorly defined and have not been directly implicated in any aqueous photochemistry, their nearly ubiquitous presence should be considered in discussions of charge transfer at real oxide surfaces.

The presence of carbon contamination on $SrTiO_3$ surfaces raises the question of whether a carbonaceous species, rather than water, is oxidized during hydrogen photogeneration on Pt-free

crystals, where difficulties with detection of slow oxygen production and the low photoactivity leave the issue unresolved. Several authors (23,24) have reported photoassisted reactions between carbon and water yielding some hydrogen and CO_2. Photo-Kolbe reactions of carboxylates have also been demonstrated (25). However, neither addition of acetate to 0.08M nor an unintentional gross contamination of the 10M NaOH electrolyte with charred epoxy residue caused significant acceleration of hydrogen production in our experiments. The presence of carbon monolayers on $SrTiO_3$ shows the need for caution in evaluating photoreactions where the total product yield is on the order of one monolayer or less.

Silicon (Auger peaks at 92 and 1613 eV) appeared on $SrTiO_3$ surfaces after illumination in both NaOH (where hydrogen was produced) and in $NaClO_4$ (where no hydrogen evolution occurred). Less Si deposited from NaOH than from $NaClO_4$, but still less Si appeared after illumination in other electrolytes from which no hydrogen was evolved. It appears that high alkali cation concentrations accelerate the etching of the borosilicate reaction vessel. Surfaces illuminated in $NaClO_4$ exhibited an unusual oxygen peak shape, most clearly visible in the higher-resolution spectra of Figure 5 as the feature with an inflection point at 484.5 eV. Knotek (26) has reported a similar peak shape on a TiO_2 surface exposed to water vapor and aged *in vacuo*. The feature may be due to a peculiar form of hydroxylation or peroxidation of the surface. However, Legaré *et al.*(27) reported a strikingly similar spectrum for air oxidized silicon and ascribed this peak to a bulk plasmon in SiO_2. The ambiguity in this data produced by silicon contamination is indicative of the problems encountered in the use of glassware with highly concentrated electrolytes. Some advantages may be found in the use of adherent thin films of electrolytes.(12)

III-3. Metallic Impurities and Surface Metallization. Kraeutler and Bard (28) have demonstrated that metal ion impurities in aqueous electrolytes readily plate out on illuminated TiO_2. No heavy metal contaminants were observed on $SrTiO_3$ surfaces illuminated in the electrolytes used here, though surface coverages less than 1% of a monolayer would have remained undetected. When H_2PtCl_6 was added to a concentration of $4x10^{-4}M$ (2000 monolayers Pt in solution) in 30% NaOH and a stoichiometric crystal was illuminated for 12 hours therein, platinum deposited unevenly onto the illuminated surface. As the Pt plated out, the rate of hydrogen evolution increased from an initial 50 monolayers /hr. to 2000 monolayers/hr. Figure 1D shows the spectrum of the thickest part of the Pt deposit, which formed around a hydrogen-containing bubble trapped under the crystal. The Auger equivalent of 3 or 4 monolayers of platinum is present. The carbon/titanium peak ratio appears significantly smaller than observed on metal-free surfaces, possibly due to carbon-consuming photoreactions (23, 24) or selective deposition of Pt on carbon.

Reducible oxides such as TiO_2 and $SrTiO_3$ have been shown to exhibit strong metal-support interaction effects in a number of catalytic reactions(29). It is possible that direct metallization of oxide semiconductors may lead to somewhat different chemistry from that obtainable with discrete oxide and metal electrodes. Bahl *et al.*(30) have undertaken photoemission studies of platinized $SrTiO_3$ surfaces and have found *in vacuo* evidence of partial negative charge transfer from $SrTiO_3$ to each surface Pt atom. Under more severe conditions intermetallic compounds may form.(13) Figure 6 shows the Auger spectrum of about 12 monolayers of Pd evaporated onto vacuum-reduced TiO_2. Both the titanium and oxygen Auger signals are almost completely masked by the overlying Pd. Upon annealing above 700°C the Ti, but not the O, signal grows indicating a diffusion of Ti to the surface. The Ti peak shape is more metallic in character than that seen on clean TiO_2. The Ti diffusion is more pronounced on Ar-sputtered surfaces with a high Ti^{3+} concentration and is not observed for Au on TiO_2 or Pd on α-Al_2O_3.

Figure 7 shows a schematic representation of low energy electron diffraction patterns on the TiO_2(110) and the vicinal (320) " stepped" surfaces. The pattern in Figure 7A was obtained after annealing a Pd film on either surface at ∿500°C; spots due to the substrate and to (111)-faced Pd crystallites were observed.The pattern in 7B developed on the stepped surface after annealing at higher temperature; superimposed on the patterns due to the substrate and Pd(111) is another set of spots whose lattice parameter is consistent with the hexagonal basal plane of a known intermetallic compound, Pd_3Ti.(31) It is not yet clear whether such metal-metal oxide reactions can be stimulated photochemically. Such reactions could modify the photoelectrochemical properties of the system, as platinum-niobium intermetallics have proven superior to pure platinum for the electrocatalysis of oxygen reduction at elevated temperatures.(32)

III-5. Comparison of Hydrogen Production with Current Measurements. To allow direct comparison of hydrogen evolution results from stoichiometric metal-free crystals in aqueous electrolyte with rates obtained from a photoelectrochemical cell, discrete $SrTiO_3$ and platinized platinum electrodes were mounted in the vacuum reaction flask. The $SrTiO_3$ electrode was prepared from a crystal polished with 1μ diamond paste, etched in molten NaOH, and reduced 4 hours in hydrogen at 1270 K. Contact was made through Ga-In eutectic and silver epoxy, and the contact was insulated with UHV-grade epoxy. Current measurements were made via the voltage drop across an 11Ω resistor placed across the electrical vacuum feedthroughs to which the electrodes were attached. Figure 9 shows the results of simultaneous measurements of integrated photocurrent and hydrogen accumulation, as measured with the gas chromatograph, in NaOH electrolytes of varying concentration.

The same trend of increasing photoresponse with increasing hydroxide concentration is seen in both measurements, showing that the hydroxide dependence of hydrogen production is not simply an artifact of the greater solubility of hydrogen in less concentrated solutions preventing escape of photogenerated hydrogen to the gas phase. However, some of the discrepancies between current and hydrogen measurements in dilute solutions may be due to this solubility factor. The role of dissolved oxygen and hydrogen in altering the effective "Fermi level" of the solution (33) has not yet been thoroughly investigated. Although oxygen is much less soluble in concentrated than in dilute NaOH solutions, it also diffuses much less rapidly at higher OH^- concentrations.(34) The relative oxygen concentrations in solutions of variable OH^- concentration deaerated by vacuum pumping (as used here) or by argon or nitrogen purging for finite times remain undetermined.

III-6. Stoichiometry of Vacuum Prepared vs. Water-dipped $SrTiO_3$. All of the Auger spectra in Figures 2, 3, and 5 were taken after rinsing the crystal in triple distilled water to remove electrolyte residue which would interfere with Auger analysis. Figure 9 shows the changes wrought upon an Ar^+ sputtered $SrTiO_3$ surface prepared *in vacuo* (A), upon exposure to room air for two minutes (B), or after a one minute rinse in triple distilled water (C). The vacuum-prepared surface, with or without air exposure, shows a higher Sr (68 eV/Ti 383 eV) ratio (0.5) than is seen in the surface exposed in liquid water (0.2). Tench and Raleigh (35) showed that immersion in water also removed Sr from $SrTiO_3$ cleaved in air. The effect is too large to be accounted for as differential attenuation by the carbon monolayer. The higher Sr concentration of the vacuum-prepared surface should lead to a lower surface electron affinity, giving electrons in the conduction band under flat-band conditions (which are likely on strongly illuminated, Pt-free crystals) greater reductive power than would be attainable at the water-dipped surface. Since rinsing in water can change the stoichiometry of vacuum-prepared crystals, it is possible that this rinsing step may obscure reversible changes in surface stoichiometry which occur during immersion and/or illumination in diverse electrolytes. The use of volatile electrolytes or gas-phase reactants is thus desirable.

III-7. Hydrogen Photogeneration from Low-Pressure Water Vapor. Water vapor can react with oxygen vacancies of illuminated pre-reduced $SrTiO_3$ surfaces to yield hydrogen and lattice oxide.(14) Vacuum-prepared (111) surfaces of pre-reduced and stoichiometric $SrTiO_3$ were heated to 400°C in 10^{-7} Torr D_2O in a UHV system equipped with a quadrupole mass spectrometer. Illumination of the pre-reduced crystal caused an increase in the D_2 pressure of the system equivalent to D_2 production of 3 monolayers/hr. No such effect was seen on the stoichiometric crystal.

Electron energy loss spectra showed that the surface Ti^{3+} concentration was smaller during illumination in water vapor than during dark exposure to water vapor. In 10^{-8} Torr D_2O photoproduction of HD, but not D_2 was observed. At crystal temperatures below 200°C photoproduction of neither D_2 or HD could be measured. No molecular or atomic oxygen photogeneration was observed under any conditions. In the absence of D_2O, heating the pre-reduced crystal to 400°C caused the slow evolution of hydrogen from the pre-reduced bulk, but no photoeffects were seen in the absence of water vapor. Both oxygen vacancies and hydrogen appear to diffuse towards the surface at 400°C. An oxygen diffusion coefficient of $7\times10^{-12}cm^2S^{-1}$ (obtained by extrapolating the data of Paladino (36) to 400°C) would allow 3×10^{13} oxygen vacancies-cm^2S^{-1} to reach the surface initially from a crystal with a bulk vacancy concentration of $10^{19}cm^{-3}$. This rate seems adequate to account for the lack of gas-phase oxygen production in this experiment. No hydrogen photoproduction was observed on pre-reduced crystals near room temperature in water vapor at up to 20 Torr pressure.(12)

IV. Discussion

IV.1 Hydrogen Production on Metal-free Crystals. Hydrogen is photogenerated on metal-free, as well as 'platinized' $SrTiO_3$ crystals in aqueous alkali electrolytes. The use of electrolytes of higher purity did not significantly decrease the rate of hydrogen production. Similar results were obtained in the adherent electrolyte films in which the total amount of metallic impurities was several orders of magnitude less than in the bulk liquid electrolyte.(12) Hydrogen photoproduction was observed from the more rigorously Pt-free crystals exposed to water vapor. While a catalytic role for very low levels of metallic impurities can not be ruled out, it appears that the clean oxide surface does have some residual activity. Weber (37) has reported Tafel plots for hydrogen evolution on anodized sodium tungsten bronze, another perovskite semiconductor, under conditions carefully designed to prevent platinum contamination. On this material currents equivalent to hydrogen photoproduction on metal-free $SrTiO_3$ ($\sim$2μA) required an overpotential of 150 mV. As this is less than the difference between the flatband potential of $SrTiO_3$ and the hydrogen redox level (2) it is quite possible that the SrTiO3 itself has sufficient catalytic activity to account for the observed production.

During hydrogen evolution on metal-free $SrTiO_3$ photogenerated electrons must diffuse to the surface against an electric field within the depletion layer which tends to drive electrons into the crystal bulk. Krauetler and Bard (25) have proposed the existence of shallow surface electron traps to account for reductive chemistry on n-type oxides. The only electron-trapping surface species as yet identified by UPS on $SrTiO_3$ or TiO_2 is the

Ti^{3+} state. Though it has been impossible to monitor this state at the liquid-solid interface, the Ti^{3+} concentration decreases during hydrogen producing illumination in water vapor. One would expect an increase in Ti^{3+} upon illumination if photopopulation of this electron trap state controlled the reaction rate. It thus appears that even on metal-free $SrTiO_3$ conduction-band electrons are the primary reductants. Since similar reaction rates occur on pre-reduced and stoichiometric crystals with disparate depletion layer widths, the electrons do not tunnel through the depletion layer. With no Pt to provide an outlet for electrons at potentials far positive of the flatband potential, strong illumination would flatten the bands almost completely and allow electrons to reach the semiconductor surface. The presence of both electrons and holes at the surface could lead to unique chemistry as well as high surface recombination rates.

On stoichiometric crystals diffuse platinization of the illuminated surface accelerated hydrogen production, while platinization of dark areas had little effect. Short diffusion distances for electrons (and/or possibly hydrogen atoms) between $SrTiO_3$ and Pt centers are beneficial to hydrogen production. Since addition of platinum, a good hydrogen evolution catalyst, does not alter the hydroxide concentration effect, the effect bears on oxygen, rather than hydrogen production.

V-2. The Hydroxide Concentration Effect. The higher rates of hydrogen evolution obtained in highly concentrated alkaline electrolytes are not predicted by simple photoelectrochemical theory since the pH dependence of the flatband potential is expected to be the same as that of the hydrogen and oxygen redox potentials.(2) Although the photoresponse of $SrTiO_3$ PEC cells have been shown to be independent of electrolyte pH (2), these measurements were taken at a high applied potential. Kawai and Sakata (38) have found that pH-related differences in the dynamic response to pulsed light of TiO_2 electrodes disappear upon application of an external anodic potential. At zero applied potential surface recombination is more rapid, and the speed of transfer of charge carriers to the solution may become critical to the conversion efficiency of the system. Small changes in band bending due to specific chemical effects would also be more important at zero applied potential.

pH-Dependent changes in surface stoichiometry could increase band bending by decreasing the electron affinity of the surface, as probably occurs during Ar^+ sputtering. However, no such stoichiometry changes have been observed by Auger, and more purely kinetic explanations of the hydroxide effect should be considered.

That rate-limiting step in oxygen production may be (1) absorption of a facile hole-acceptor species, (2) hole transfer to an absorbed or electrolyte species, or (3) desorption of oxidized products. These steps must compete with bulk and surface recombination processes. Williams and Nozik (39) have shown that

step (2) is likely to be highly irreversible and the solid-liquid interface, casting doubt onto whether step (3) could be rate controlling. Comparison of the conditions required for hydrogen photogeneration from aqueous electrolytes and from low pressure water vapor may shed some light on steps (1) and (2).

Hydrogen photogeneration from 10^{-7} Torr water vapor occurs only on pre-reduced crystals at elevated temperatures where a stoichiometric reaction with reduced centers (Ti^{3+}-Vo^{-}) from the crystal bulk is possible. These oxygen vacancies could react with zero valent oxygen produced at the surface in a reaction analogous to that yielding $O_{2(g)}$ in aqueous solution. Alternately, the oxygen from water may never be oxidized above the -II or -I state, and holes may be directly accepted by the reduced center. Figure 10 shows the energies of known surface species (from UPS spectra (22)) and estimates of the filled state distribution of several aqueous species (17) relative to the $SrTiO_3$ band edges. All of the UPS-detectable hydroxide states formed upon adsorption of low pressure water vapor lie well below the band edge, where neither thermalized nor somewhat hot holes could be accepted. On the clean, water vapor exposed surface only the Ti^{3+} species could accept holes, though considerable relaxation of the hole must occur. Oxidation of Ti^{3+} is, in fact, observed upon illumination. The filled state distribution of aqueous OH^{-} is believed to overlap the $SrTiO_3$ valence band edge, and rapid isoenergetic hold transfer is possible, leading to the catalytic oxidation of water. At high electrolyte concentrations hydroxide-hydroxide reactions may increase the overlap, thereby facilitating hole transfer. If the aqueous energy levels are as shown, no adsorbed surface species would be needed to mediate charge transfer, though carbon states are available at the proper energy.

It should be noted that while UPS could not detect an adsorbed hydroxide species with surface coverage less than 10% of a monolayer, such a species could be chemically active. The same hole-acceptor could be present at both the gas-solid and liquid-solid interface, but the rate of its formation may be inadequate to compete with oxygen diffusion into the bulk from the gas-solid interface. Munuera (40) has found that measurable rates of restoration of a hydroxyl species linked to the photoactivity of TiO_2 powders for oxygen desorption require treatments harsher than immersion in liquid water.

IV-3. Summary. No Auger detectable changes in surfaces composition correlate with the higher rates of hydrogen photogeneration on metal-free $SrTiO_3$ observed in highly concentrated aqueous alkaline electrolyte. Platinized crystals and PEC cells show similar enhancement of photoactivity at high hydroxide concentrations. Although no hydrogen photogeneration is seen from water vapor at pressures up to 20 Torr on crystals near room temperatures, hydrogen photogeneration does occur on pre-reduced crystals at temperatures where oxygen diffusion into the bulk is

rapid. Kinetics of hole-transfer or hydroxylation may determine the overall reaction rate at zero applied potential. Carbon states lying within the $SrTiO_3$ forbidden gap may mediate charge transfer in some photochemical reaction systems, and intermetallic compound formation may alter the catalytic properties of directly metallized titaniferous semiconductors.

Acknowledgement

This work was supported by the Division of Chemical Sciences, Office of Basic Energy Sciences, United States Department of Energy under Contract No. W-7405-ENG-48. The authors would like to thank Dr. John Wang for assistance with the scanning Auger microprobe and Dr. Phillip Ross for the use of his Auger apparatus.

Literature Cited

1. Fujishima, A., Honda, K., Bull. Chem. Soc. Jpn., 1971, 44, 1148
2. Wrighton, M.S., Ellis, A.B., Wolczanski, P.T., Morse, D.L., Abrahamson, H.B., Ginley, D.S., J. Am. Chem. Soc. 1976, 98, 2774.
3. Mavroides, J.G., Kafalas, J.A., Kolesar, D.F., Appl. Phys. Lett. 1976, 28, 241.
4. Bard, A.J., Bocarsly, A.B., Fan, F.F., Walton, E.G., Wrighton, M.S., J. Am. Chem. Soc., 1980, 102, 3671.
5. Schrager, M., and Collins, F.C., J. Appl. Phys., 1975, 46, 1934.
6. Hurlen, T., Acta Chem. Scan., 1959, 13, 365.
7. Harris, L.A., Wilson, R.H. J. Electrochem. Soc.,1976,123,1010.
8. Frank, S.M., Bard, A.J. J. Am. Chem. Soc.1975, 97, 7427.
9. Frank, S.M., Bard, A.J. J. Am. Chem. Soc. 1977, 99, 303.
10. Wilson, R.H., Harris, L.A., Gerstner, M.E., J. Electrochem. Soc. 1979, 126, 844.
11. Nozik, J.A., Appl. Phys. Lett. 1977, 30, 567.
12. Wagner, F.T., Somorjai, G.A. J.Am. Chem. Soc. 1980, 102, 5494
13. Wanger, F.T., Somorjai, G.A. to be published.
14. Ferrer, S., Somorjai, G. A. to be published.
15. Lo, W.J., and Somorjai, G.A., Phys. Rev. B, 1978, 17, 4842.
16. Mühlebach, J., Müller, K., Schwarzenbach, G., Inorg. Chem. 1970, 9, 2381.
17. Sakata, T., Kawai, T., Ber. Bunsenges. Phys. Chem., 1979, 83 486.

18. Tomkiewicz, M., J. Electrochem. Soc., 1980, 127, 1518.
19. Haas, T.W., Grant, J.T., Dooley, G.J.III, J. Appl. Phys. 1972, 43, 1853.
20. Weber, R.E., R-D Magazine, Oct. 1972.
21. Ross, P.N., unpublished data.
22. Ferrer, S., and Somorjai, G.A., Surface Sci. 1980, 94, 41.
23. Sato, S., White, J.M., Chem. Phys. Lett., 1980, 70, 131.
24. Kawai, T., Sakata, T., Nature, 1979, 282, 283.
25. Kraeutler, B., Bard., A.J., J. Am. Chem. Soc., 1978, 100, 5985.
26. Knotek, M.L., in "Proc. Symp. on Electrode Materials and Processes for Energy Conversion and Storage," eds. McIntyre, J.D.E., Srinivasan, S., Will, G. (Proceedings, Vol. 77-6, The Electrochem. Soc., Princeton, NJ, 1977).
27. Legaré, P., Maire, G., Carriére, B., DeVille, J.P., Surface Science, 1977, 68, 348.
28. Kraeutler, B., Bard, A.J., J. Am. Chem. Soc., 1978, 100, 431F.
29. Tauster, S.J., Fung, S.C., Garten, R.L., J. Am. Chem. Soc. 1978, 100, 170.
30. Bahl, M.K., Tsai, S.C., Chung, Y.W., Phys. Rev. B., 1980, 21, 1344.
31. Nishimura, J., Hiramatsu, T., J. Japan Inst. Metal, 1958, 22, 38.
32. Ross, P.N., National Fuel Cell Seminar Abstracts, 1980, 42.
33. Memming, R., Electrochimica Acta, 1980, 25, 77
34. Gubbins, K.E., Walker, R.D., J. Electrochem, Soc. 1965, 112, 469.
35. Tench, D.M., Raleigh , D.O., in "Electrocatalysis on Non-Metallic Surfaces," NBS Spec. Pub. 455, 1976, p.229.
36. Paladino, A.E., Rubin, L.G., Waugh, J.S., J. Phys. Chem. Solids, 1965, 26, 391.
37. Weber, M.F., "Electrocatalytic Activity and Surface Properties of Tungsten Bronzes," Ph.D. Thesis, Iowa State University, 1977, p.76.
38. Kawai, T., Sakata, T., Chem. Phys. Lett. in press.
39. Williams, F., Nozik, A.M., Nature, 1978, 271, 137.
40. Mumuera, G., Rives-Arnau, V., Saucedo, A., J. Chem. Soc. Faraday Trans. I, 1979, 75, 736.

Figure 1. Hydrogen accumulation as a function of time on a stoichiometric, metal-free $SrTiO_3$ crystal in 20M NaOH.

Figure 2. Auger spectra of water-rinsed stoichiometric crystals (A) after pretreatment described in "Experimental" section, (B) after illumination in 30% (10M) NaOH (H_2 produced), (C) after illumination in 10M $NaClO_4$ (no H_2 produced), (D) after illumination in 30% (10M) NaOH with Pt(IV) added to $4x10^{-4}$ M.

Figure 3. Low beam current (<0.1μA) Auger spectra, (A) before illumination, (B) after illumination in 30% (10M) NaOH, (C) after illumination in 10M $CaClO_4$.

Figure 4. UPS spectra of clean Ar^+ sputtered $SrTiO_3$ before (A) and after (B) contamination with about 1 monolayer C in vacuo.

Figure 5. Details of oxygen Auger spectra of $SrTiO_3$ crystals, (A) Ar^+ sputtered, (B) illuminated in 7M Ω H_2O, (C) illuminated in 30% NaOH, (D) illuminated in 10M $NaClO_4$, (E) illuminated in 1M H_2SO_4. Inflection point of main oxygen peak at 501 eV.

Figure 6. Auger spectra of Pd film evaporated onto TiO_2 before and after annealing.

Figure 7. Schematic representations of LEED patterns and their real-space interpretations for Pd on TiO_2(110) and (320). Key to spots: • substrate, Δ Pd(111)-faced crystallites, ■ intermetallic crystallites.

Figure 8. Simultaneous measurements of H_2 yield and integrated current passed as a function of NaOH electrolyte concentration for a n-$SrTiO_3$/Pt PEC cell. Each vertical division corresponds to the equivalent of 1000 monolayers H_2 produced.

Figure 9. Auger spectra of (A) freshly Ar^+ sputtered surface, (B) A. exposed to room air 2 min., (C) A. exposed to 7M-Ω water one minute.

Figure 10. Filled levels of surface and aqueous species referenced to $SrTiO_3$ band edges and H_2, O_2 redox couples

Table I. Hydrogen photogeneration from stoichiometric initially metal-free, $SrTiO_3$ in various electrolytes. *prereduced crystal. 30% NaOH=10M.

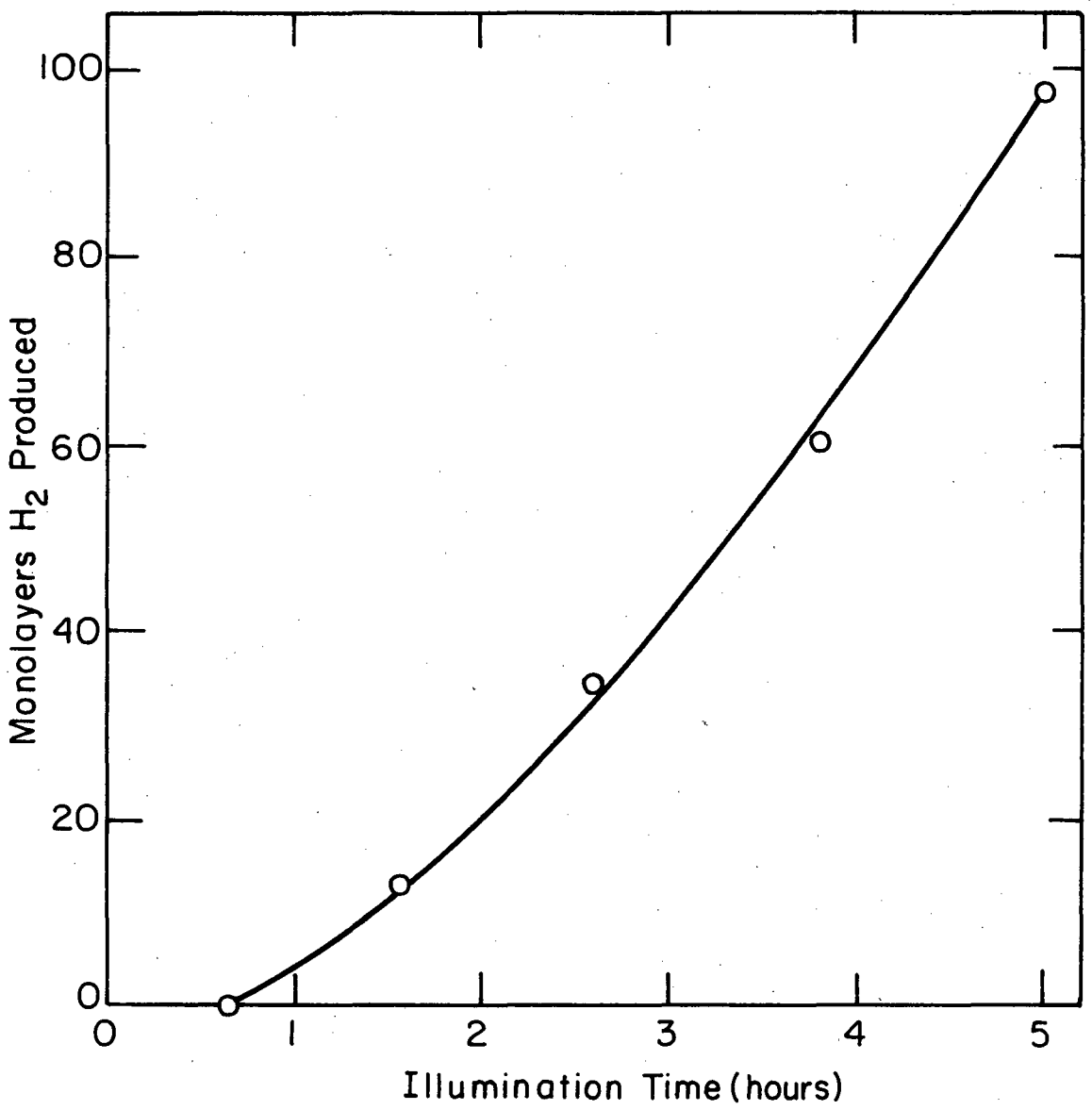
100
80
60
40
20
0
Monolayers H_2 Produced
0
1
2
3
4
5
Illumination Time (hours)
XBL 801 4602

Fig.1

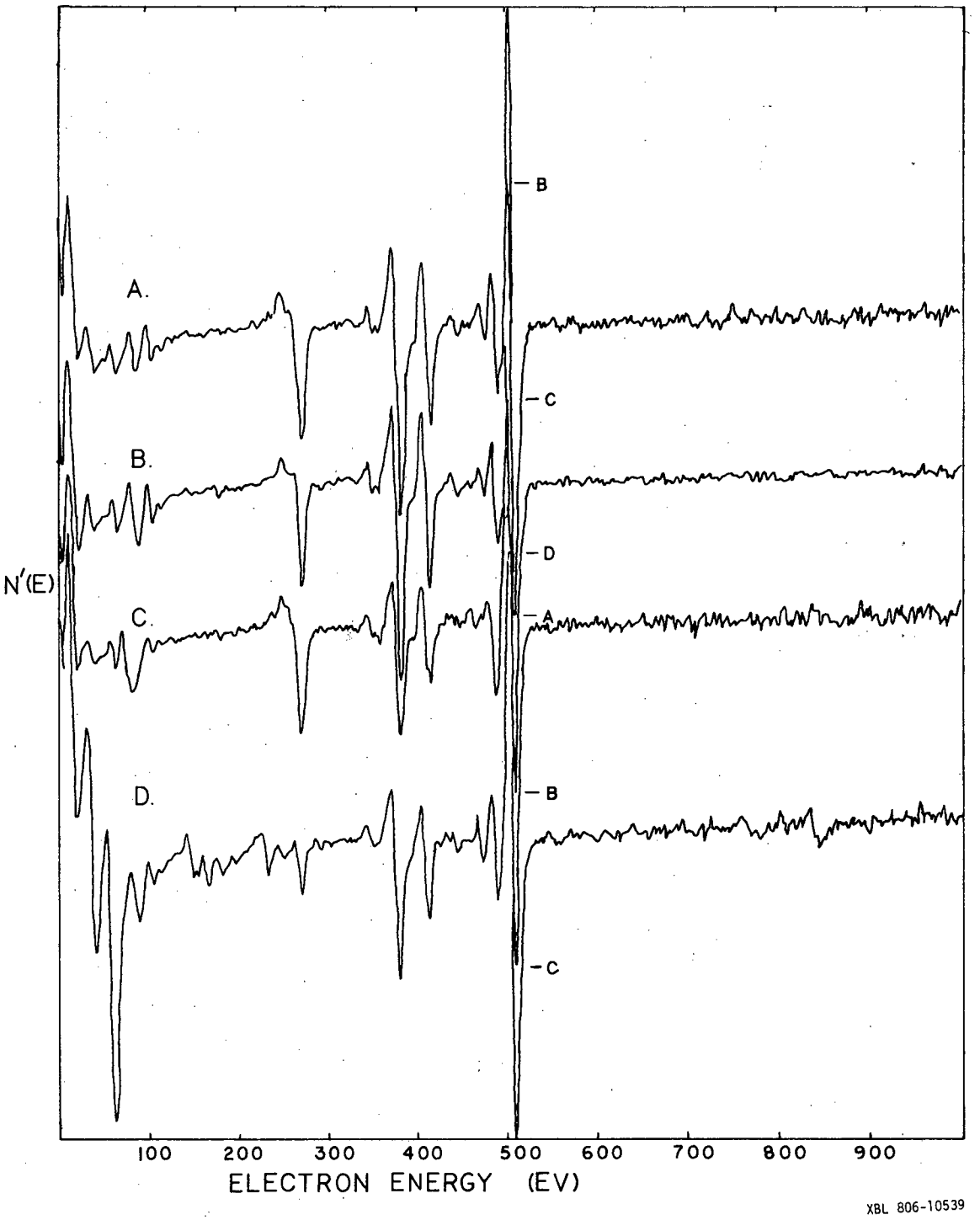
A.
B.
C.
D.
N'(E)
B
C
D
A
B
C
100
200
300
400
500
600
700
800
900
ELECTRON ENERGY (EV)
XBL 806-10539

Fig.2

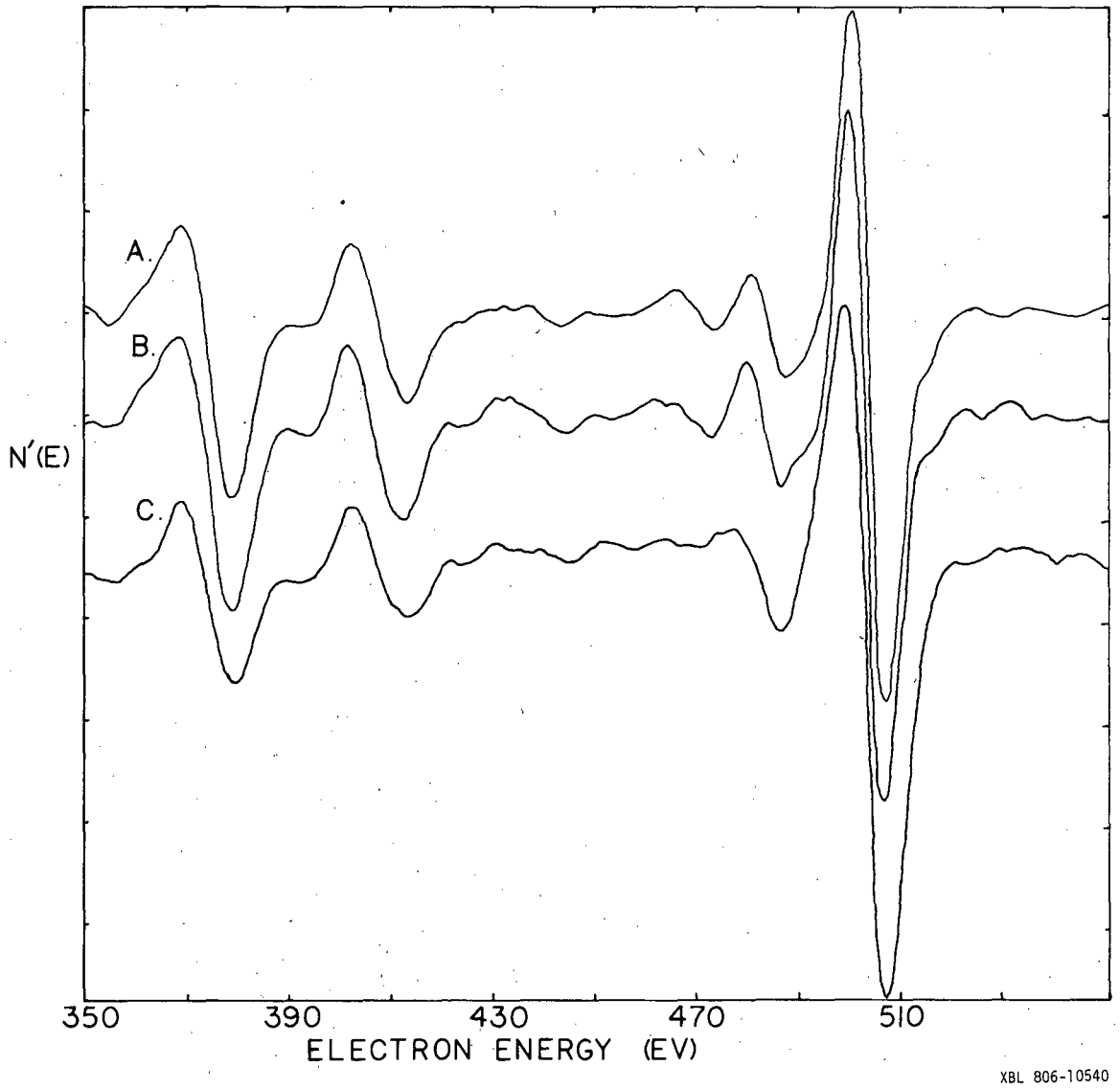

Fig.3

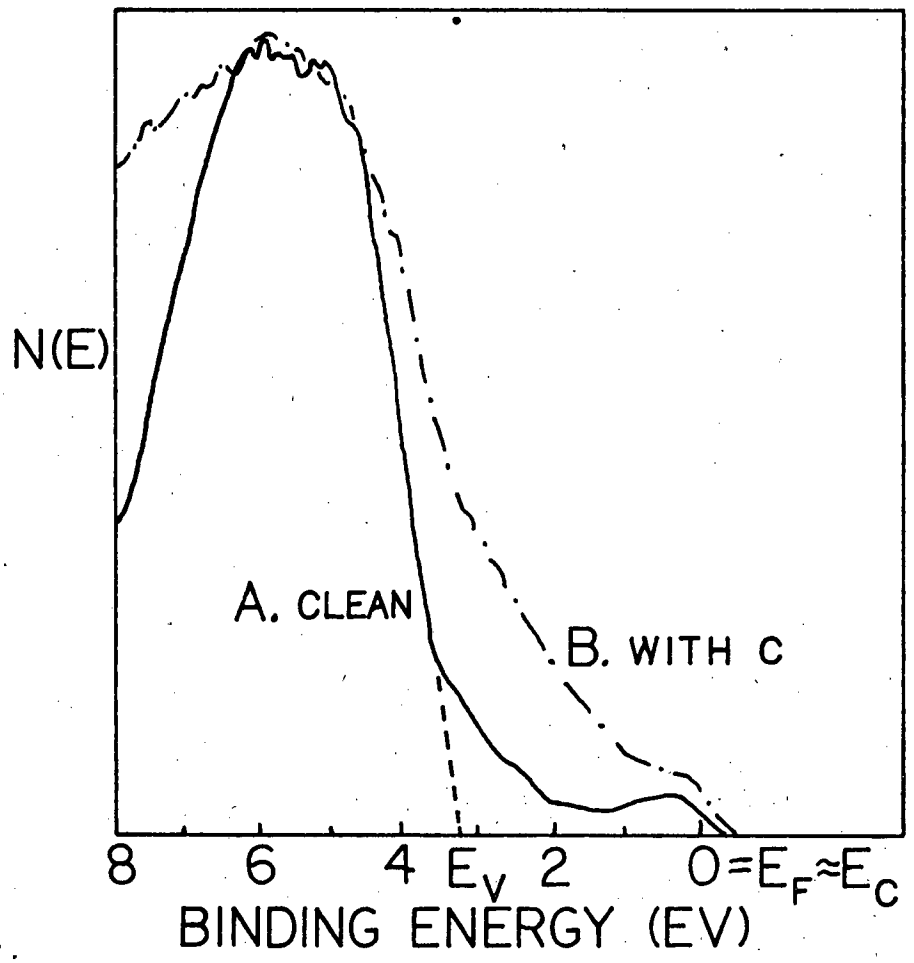

Fig.4

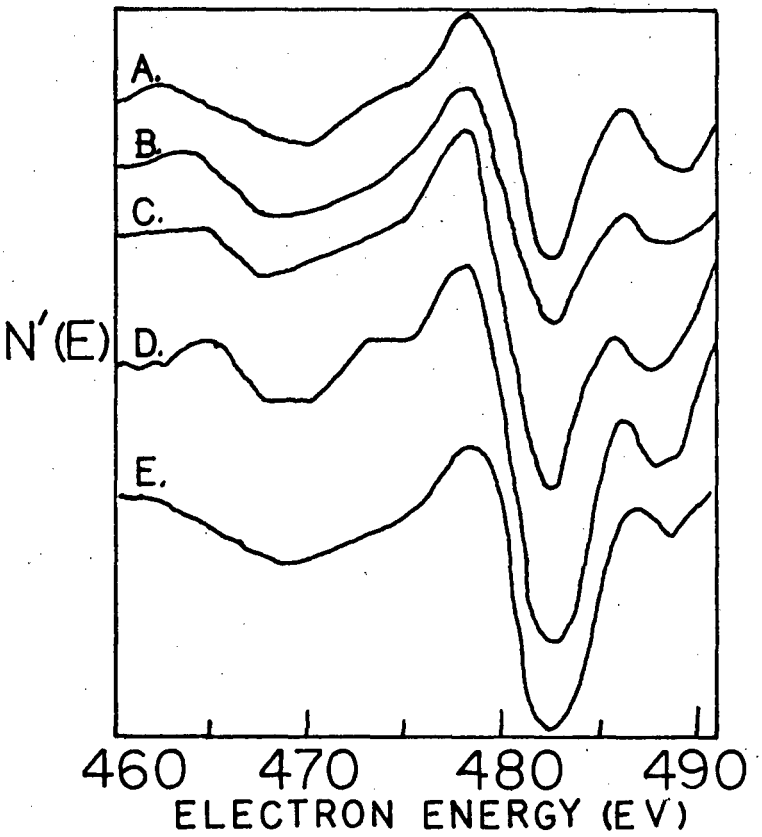

Fig.5

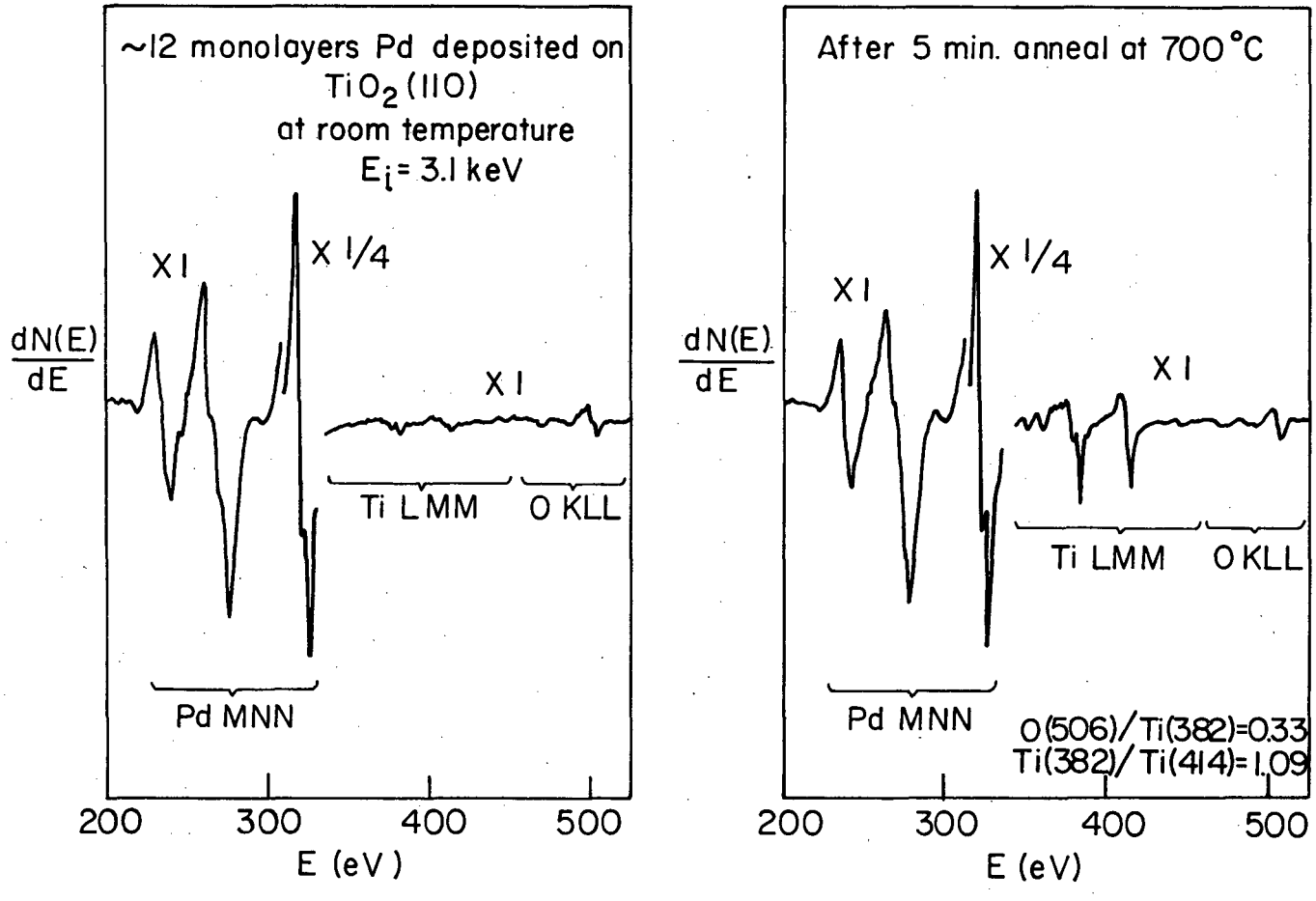

XBL 781-4464

Fig. 6

Structure A (110 and stepped)

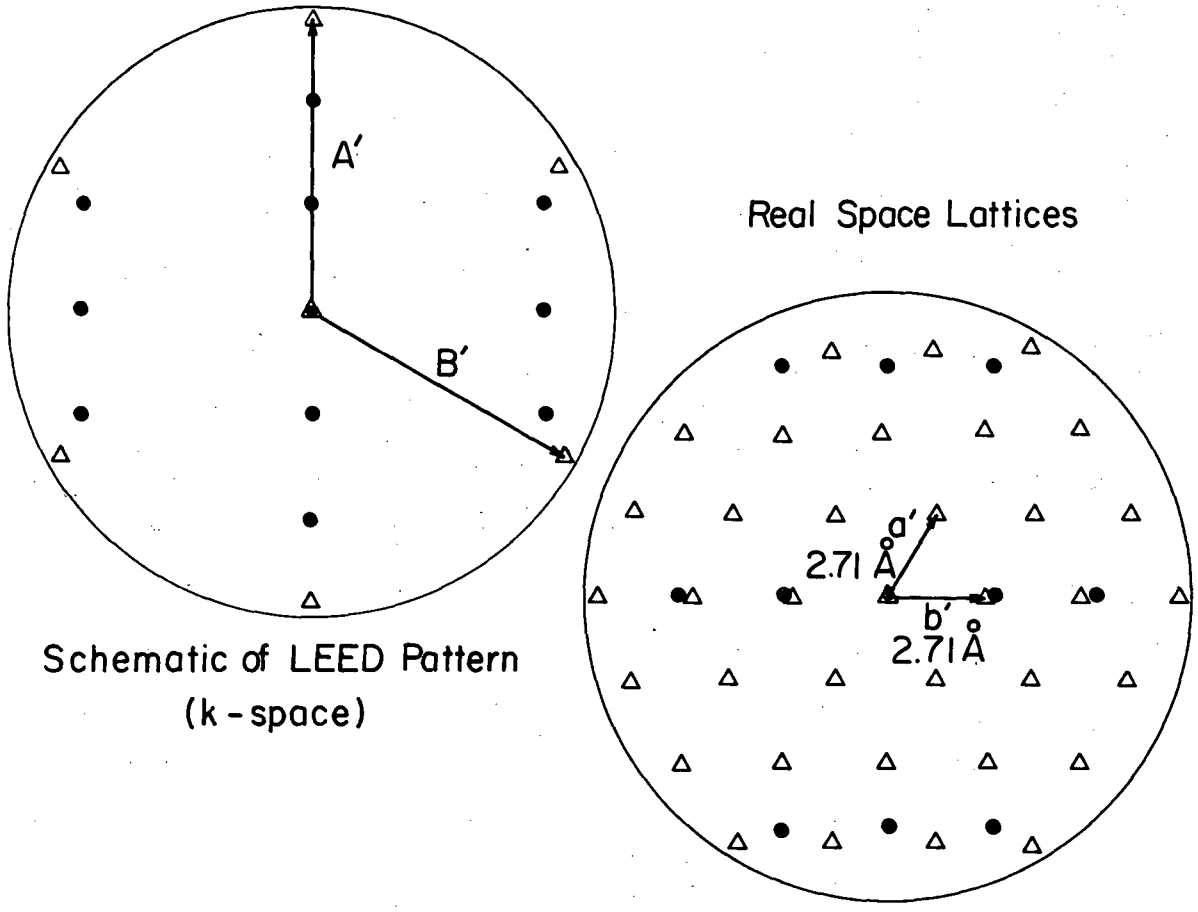

Schematic of LEED Pattern
(k-space)

XBL 781-4460

Fig. 7a

Structure B (stepped surface)

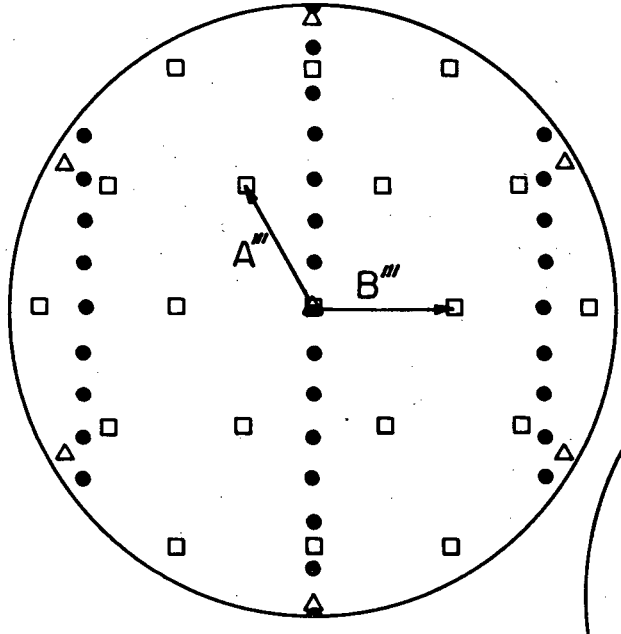

LEED Schematic
(750) TiO_2 + ~12 ml Pd
annealed at 850°C

Real Space

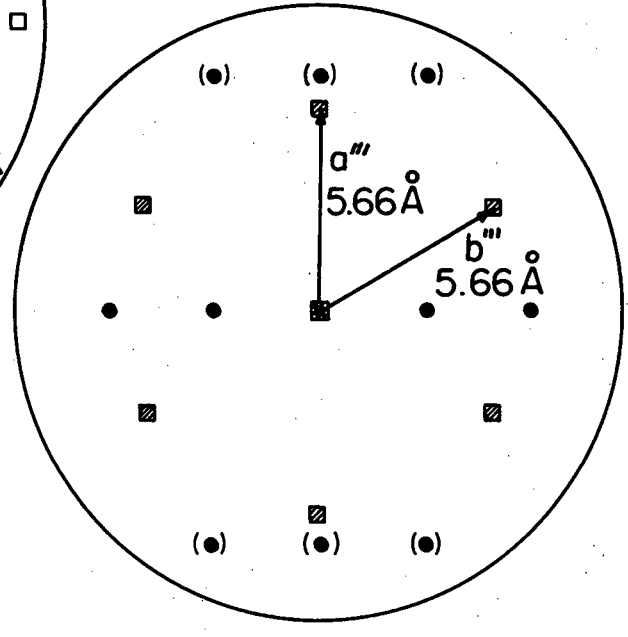

a‴ ∥ TiO_2 [1$\bar{1}$0]

XBL781-4461

Fig. 7b

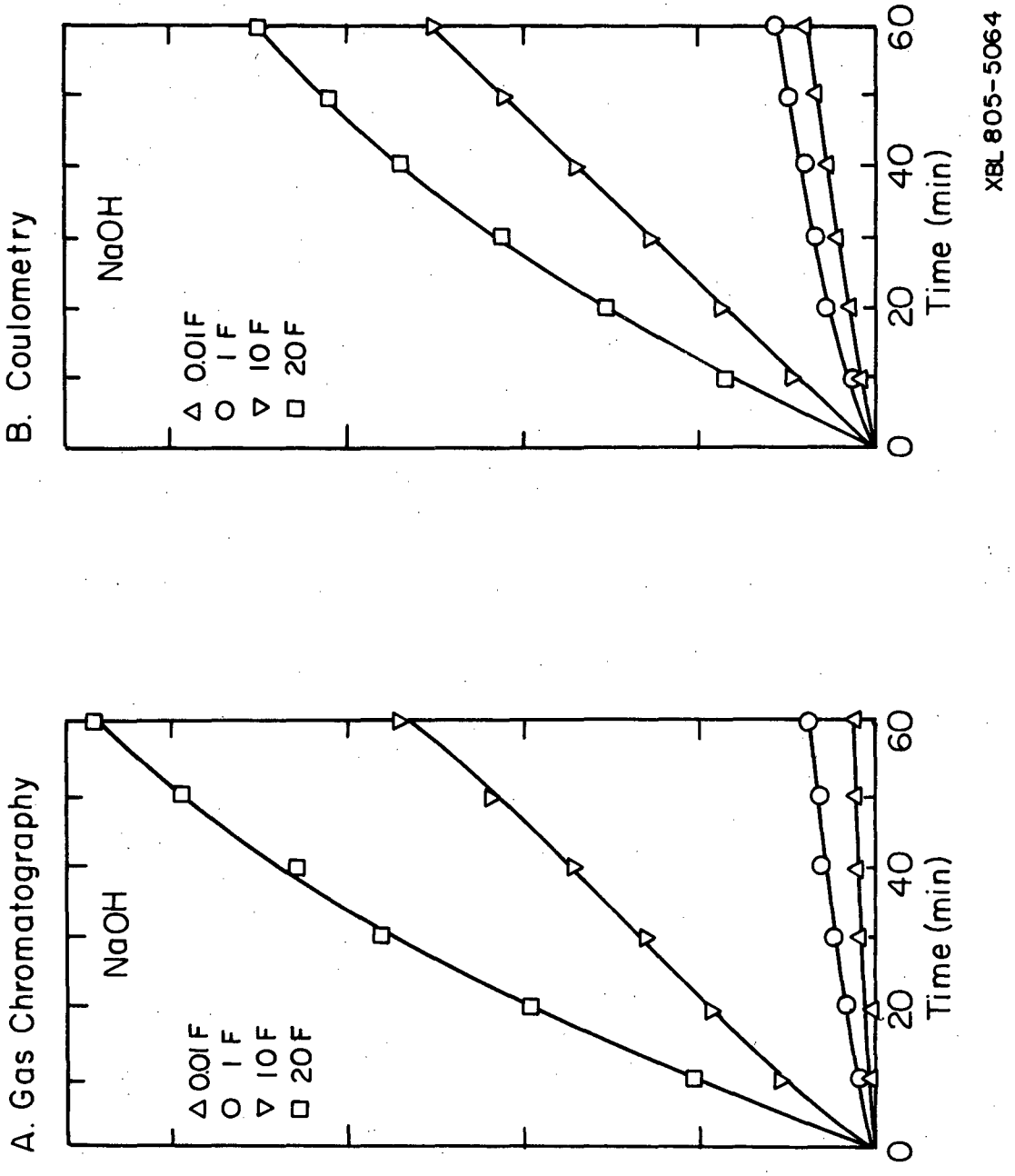
B. Coulometry
NaOH
△ 0.01F
○ 1F
▽ 10F
□ 20F
0
20
40
60
Time (min)
XBL 805-5064
A. Gas Chromatography
NaOH
△ 0.01F
○ 1F
▽ 10F
□ 20F
0
20
40
60
Time (min)

Fig.8

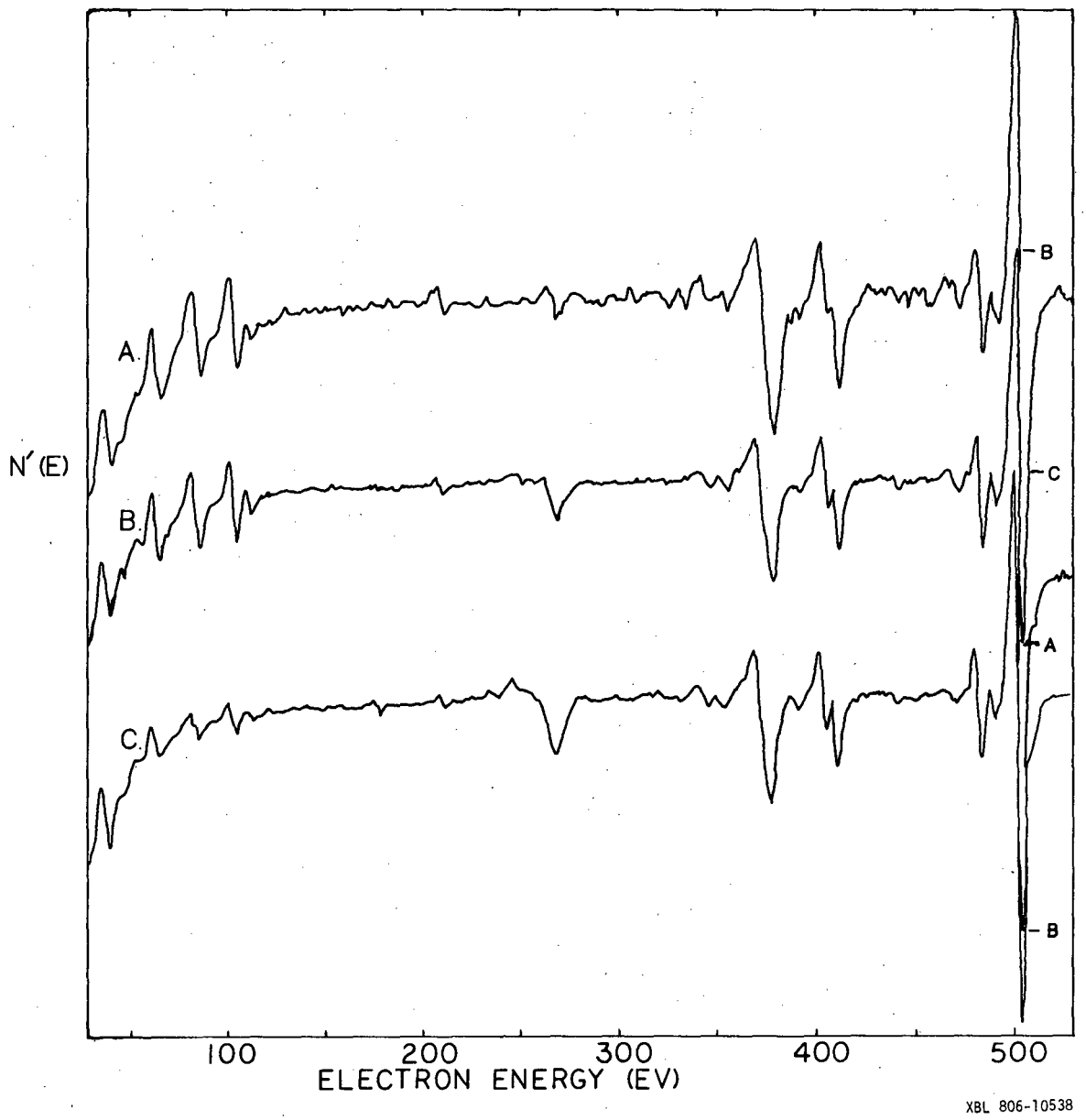
N´(E)
A
B
C
B
C
A
B
100
200
300
400
500
ELECTRON ENERGY (EV)
XBL 806-10538

Fig.9

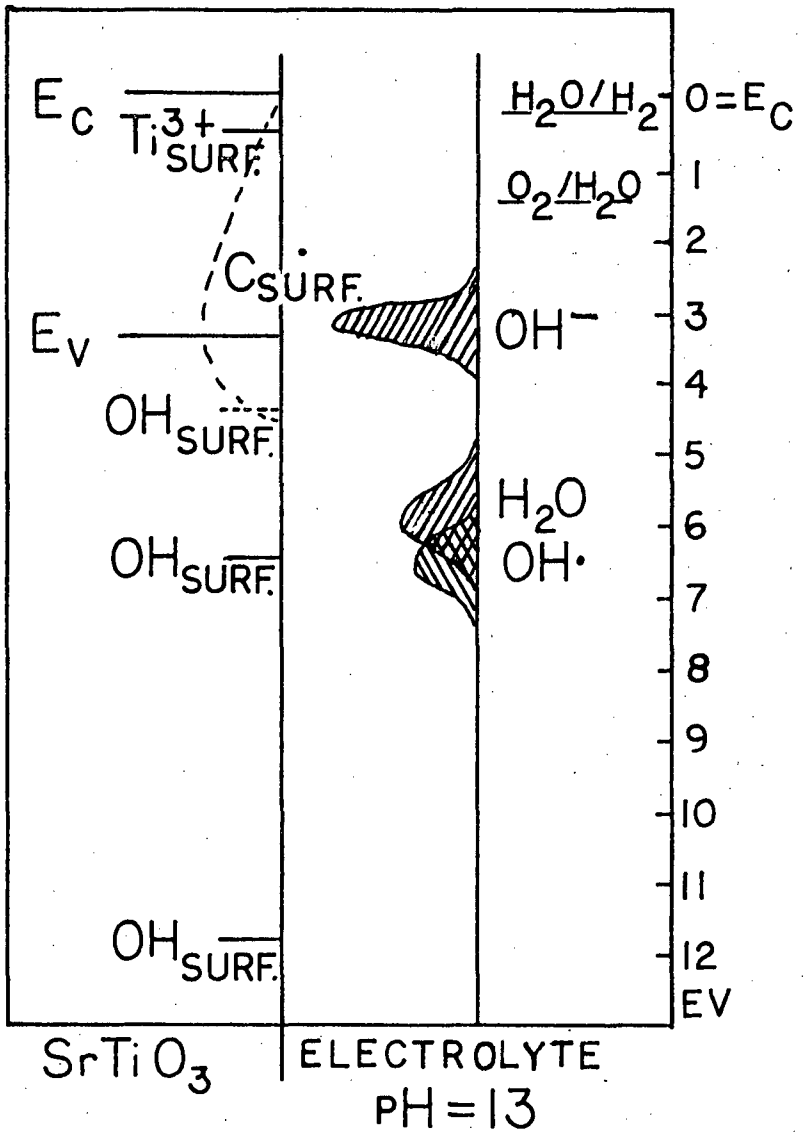
E_C
$Ti^{3+}_{SURF.}$
$C_{SURF.}$
E_V
$OH_{SURF.}$
$OH_{SURF.}$
$OH_{SURF.}$
H_2O/H_2
O_2/H_2O
OH^-
H_2O
OH·
0=E_C
1
2
3
4
5
6
7
8
9
10
11
12
EV
$SrTiO_3$
ELECTROLYTE
pH=13

Fig.10

Table I.

Electrolyte	Run duration/ Hr	Normalized H_2 yield (monolayers)	Average yield (monolayers/hr)
30% reagent NaOH	12	1300	110
30% ultra-pure NaOH	17	940	55
30% high purity NaOH, acetate added to 8×10^{-2} M	18	1250	70
30% reagent NaOH Pt(IV) added to 4×10^{-4} M	12	19,200	1600
10M reagent $NaClO_4$	24	0	0
7M-Ω water	13	36	3
1M H_2SO_4	15	0	0
40% reagent NaOH	10	600	60

This report was done with support from the Department of Energy. Any conclusions or opinions expressed in this report represent solely those of the author(s) and not necessarily those of The Regents of the University of California, the Lawrence Berkeley Laboratory or the Department of Energy.

Reference to a company or product name does not imply approval or recommendation of the product by the University of California or the U.S. Department of Energy to the exclusion of others that may be suitable.

TECHNICAL INFORMATION DEPARTMENT
LAWRENCE BERKELEY LABORATORY
UNIVERSITY OF CALIFORNIA
BERKELEY, CALIFORNIA 94720